

Coherent combining of diode laser beams in a master oscillator – zigzag slab power amplifier system

A.P. Bogatov, A.E. Drakin, G.T. Mikaelyan

Abstract. An integrated zigzag laser diode amplifier, with each segment (zigzag) consisting of three sections, is considered. The operation of this amplifier is analysed. It is shown that the presence of three sections with independent pump currents makes it possible to combine coherently all amplifier output beams. The first two sections in this configuration play the role of a phase shifter, and the third serves as a power amplifier. The influence of fluctuations of the output radiation phase in each segment on the resulting brightness of total output beam of the entire amplifier is investigated.

Keywords: diode optical amplifier, coherent beam combining.

1. Introduction

Currently, the diode laser is one of the most widespread types of lasers that are used in practice. Due to the high research intensity of diode lasers, they can be constantly upgraded using new technologies. The most urgent line of research in this field is aimed at increasing their output power. Specifically in this parameter diode lasers may be (and are) inferior to lasers of other types. Concerning the studies in this field, the investigations devoted to combining coherent beams from individual diode lasers appear to be especially promising. In particular, the most convenient method of forming many mutually coherent beams is the use of systems of amplifiers with radiation from the same master oscillator applied to their inputs.

The master oscillator–power amplifier (MOPA) system with a common optical axis has been known for diode lasers, including their integrated design (see, e.g., [1–5]). In this study we consider an amplifier with a zigzag optical axis. The system consists of a single-frequency oscillator and many successive amplifiers with a spatially distributed output of amplified mutually coherent radiation at each tilt of the optical axis.

Note that interferometric devices with a zigzag beam path between two reflecting planes have been known in optics for a long time (an example is the classical version in the form of Lummer–Gehrcke plate [6]). This scheme was also applied in an optical amplifier; see, e.g., the studies devoted to a zigzag

Nd : glass slab amplifier [7]. However, a zigzag beam path was used in that amplifier version to compensate for the regular spatial inhomogeneity in the amplifier cross section rather than to implement distributed radiation output. The optical axis tilt angle in the zigzag exceeded the double total internal reflection angle. A version of a cavity zigzag diode laser with a broken optical axis and distributed radiation output was experimentally implemented in [8]; the operation of that laser was theoretically analysed in [9].

We analyse below a version of MOPA diode system, whose amplifier is most similar to the laser used in [8]. Nevertheless, despite the external similarity, there is a significant and fundamental difference between the zigzag laser and MOPA system: the cavity of such a laser with N periodically repeated segments has an equivalent optical length exceeding the optical length of one segment by a factor of N . This cavity has a system of high-density eigenmodes with different frequencies and distributed radiation output from each segment (at the optical axis tilt). The spatial distributions of saturable gain and refractive index determine which specific modes are excited in this laser and which set of phases is implemented at each output from the cavity. As a result, one meets hard-to-solve problems with coherent beam combining (which calls for strictly determined phase relations).

This is the main reason why the results of [8] cannot be applied in our analysis. In addition, the parameters of modern heterostructures with quantum-well active regions differ significantly from the structural parameters used in [8].

In this paper, we report the results of a theoretical simulation of a system composed of a master oscillator and a zigzag diode power amplifier, fabricated on the basis of modern quantum-well heterostructures.

2. Analysis of amplifier

Figure 1 shows a simplified schematic of this system, which includes two units. The first is a master oscillator based on a single-frequency diode laser with an external spectrally selective cavity, whose selective element is, e.g., a single-mode fibre with a Bragg phase grating. The second unit is a diode bar with a zigzag electrical contact and upper layers specially processed to form optical waveguiding regions (ridge-like waveguides). Thus, this diode bar is a periodic sequence of diode amplifiers in the form of N zigzags with partial radiation output from each zigzag on one of the bar faces. The other face has a highly reflective coating. A simplified schematic of one zigzag, composed of three sections, is shown in Fig. 2. The first part of a zigzag, with a negative tilt ($-\varphi_0$), is a two-section amplifier, which provides radiation phase and intensity con-

A.P. Bogatov, A.E. Drakin Lebedev Physical Institute, Russian Academy of Sciences, Leninsky prosp. 53, 119991 Moscow, Russia; e-mail: ya.bogatov47@yandex.ru;
G.T. Mikaelyan Lassard systems, Kievskoe sh. 74, 249032 Obninsk, Moscow region, Russia

Received 26 June 2019
Kvantovaya Elektronika 49 (11) 1014–1018 (2019)
Translated by Yu.P. Sin'kov

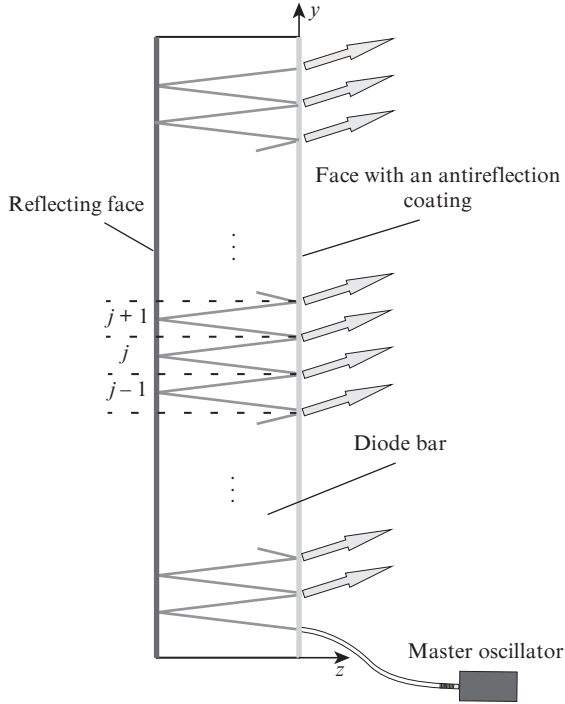


Figure 1. Schematic of an integrated zigzag optical amplifier with a master oscillator.

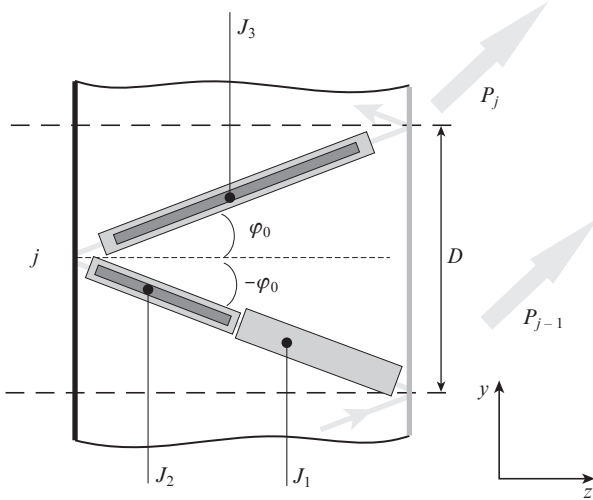


Figure 2. Schematic of a three-section optical amplifier, forming one segment (zigzag) of the integrated amplifier: j is the segment number; φ_0 is the tilt angle of the sections to the z axis; and J_1, J_2 , and J_3 are the pump currents of the sections.

trol. The second part, with a positive tilt (φ_0) with respect to the normal to the output face, is the third section of the amplifier, which serves as an output power amplifier.

The difference in the section designs is related to the planar technology of optical confinement in the plane parallel to the structure layers. This difference is as follows: the first section has a much larger waveguide value of the phase–amplitude coupling coefficient R_1 than the two other sections (with coefficients R_2 and R_3); for example, the first-section waveguide is a gain-guided one, while the waveguides of the two other sections are index-guided ones, which can be fabricated, for example, similar to the design described in [10].

When analysing the amplifier operation, we will use the dimensionless radiation intensity, normalised to the saturation intensity: $u(z) = I(z)/I_s$, where $I_s = \hbar\omega/(\sigma\tau)$, $\hbar\omega$ is the photon energy, σ is the stimulated emission cross section; and τ is the spontaneous recombination time of carriers. An input beam with an intensity $u_0^{(1)}$, having passed through the first two parts (preliminary amplification stage) of the first zigzag, reaches its third part (power amplifier), and then arrives at the bar output face, thus forming two beams: an output beam with intensity $u^{(1)}$ and a reflected beam with intensity $u_0^{(2)}$; the latter beam is an input beam for the second zigzag. The process is repeated in the second zigzag and leads again to the formation of two beams: output, with intensity $u^{(2)}$, and reflected, with intensity $u_0^{(3)}$, which is an input beam for the third zigzag. The same occurs in the next zigzags. As a result, a combined beam is formed on the output face (within the bar), which consists of N individual beams with intensities $u^{(1)}, u^{(2)}, \dots, u^{(N)}$. We will analyse the operation of this system using the results of [11].

Let us consider one zigzag (e. g., with number j) (Fig. 2). The working point of its three sections is set by the values of the three currents through them (J_1, J_2, J_3). It will be shown below that, varying these currents, one can tune independently the output beam phase and intensity, which is necessary for subsequent coherent combining of beams from different zigzags. According to [11], the intensities of the input and output beams in the j th zigzag are related by the system of transcendental equations

$$\begin{aligned} \frac{v_1}{u_0^{(j)}} \left(\frac{g_1 - u_0^{(j)}}{g_1 - v_1} \right)^{g_1+1} &= \exp(g_1 \alpha l_1), \\ \frac{v_2}{v_1} \left(\frac{g_2 - v_1}{g_2 - v_2} \right)^{g_2+1} &= \exp(g_2 \alpha l_2), \\ \frac{u^{(j)}}{v_2} \left(\frac{g_3 - v_2}{g_3 - u^{(j)}} \right)^{g_3+1} &= \exp(g_3 \alpha l_3). \end{aligned} \quad (1)$$

Here,

$$g_k = (G_k - \alpha)/\alpha; \quad G_k = \frac{\Gamma_k \sigma \tau (J_k - J_{tr}^k)}{e d_a W_k l_k}; \quad k = 1, 2, 3;$$

v_1 and v_2 are the dimensionless output intensities in the first and second zigzag sections, respectively; α is the nonresonant loss factor; e is the elementary charge; and d_a is the total thickness of active region. For each k th zigzag section, g_k is the dimensionless gain, G_k is the mode gain, J_k is the pump current, J_{tr}^k is the transparency current, Γ_k is the optical confinement factor (for two transverse directions), W_k is the width of the pumped region, and l_k is the section length. The variable part ξ of the phase difference for the output and input beams is found from the equation

$$\xi = -\frac{R_1}{2} \ln \left(\frac{v_1}{u_0^{(j)}} \right) - \frac{R_2}{2} \ln \left(\frac{v_1}{v_2} \right) - \frac{R_3}{2} \ln \left(\frac{u^{(j)}}{v_2} \right), \quad (2)$$

where R_k is the mode phase–amplitude coupling coefficient for the k th section.

The most interesting case is where all output intensities are equal to each other. Obviously, to implement it, the following matching condition must be satisfied for each j th zigzag:

$$u_0^{(j+1)} = u^{(j)}r = u_0, \quad u^{(j)} \equiv u, \quad (3)$$

where r is the output face reflectance. Equation (3) implies equality of intensities of all input beams and the same for the output beams at a complete gain $K = 1/r$ for all three zigzag sections. It can easily be seen that the number of independent variable parameters entering (1)–(3) exceeds the number of equations; therefore, one can always choose them so as to simultaneously satisfy condition (3) and, varying the currents J_1 and J_2 (and, correspondingly, g_1 and g_2), change the output radiation phase by a value $\Delta\xi$ that is much larger than 2π . Figure 3 presents a calculated dependence of $\Delta\xi$ on the currents J_1 and J_2 . In the case of the constant pump current J_3 for the third section, this dependence provides constant intensities u_0 and u of the input and output beams. The parameter values used in the calculation are listed in Table 1.

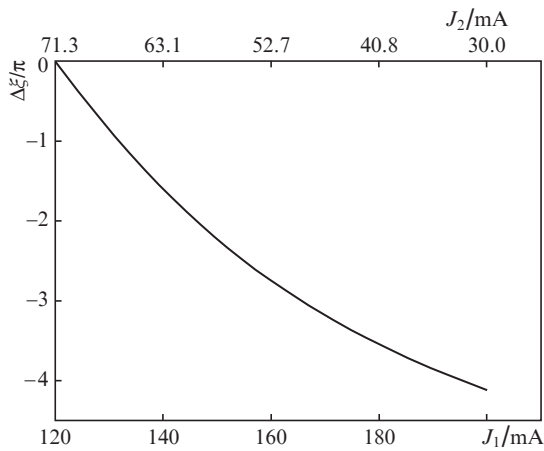


Figure 3. Phase change $\Delta\xi$ for the output radiation of an individual segment at a simultaneous change in the pump currents J_1 and J_2 of the first two sections of this segment. The output power $P_0 = 1$ W, the pump current of the third section is $J_3 = 0.72$ A, and the input radiation power for the first section is 10 mW.

Thus, the first two zigzag sections play the role of not only an amplifier but also of a phase shifter, which is due to the presence of a section with a phase–amplitude coupling coefficient R greatly exceeding the corresponding coefficients for the other sections. In the case under consideration, this is the first section with a horizontal gain-guided waveguide, the R value of which, according to [12], may be anomalously large ($R_1 = 12$).

The vertical waveguide (with a transverse distribution of the refractive index along the x axis) in the overwhelming majority of diode lasers and amplifiers is formed by heterostructure layers and maintains only one fundamental transverse mode with practically invariable amplitude distribution. For another transverse direction [horizontal, lying in the (yz) plane], special measures must be taken to form a waveguide. For example, a heterostructure with ridge-shaped upper layers can be used [13]. We will proceed from the geometry of diode amplifiers possessing this horizontal waveguide for at least two sections, including the output amplifier, and assume that the parameters of this waveguide allow it to maintain the propagation and amplification of only one fundamental transverse mode with an effective width w . Then we restrict ourselves to the consideration of only the two-dimensional

Table 1. Power amplifier parameters used for calculation.

Parameter	1st section, gain-guided	2nd section, index-guided	3rd section, index-guided
Differential gain (stimulated-emission cross section) $\sigma/10^{-15} \text{ cm}^2$	0.4	1.0	1.0
Loss factor α/cm^{-1}	15	0.8	0.8
Active-region transparency density $N_{tr}/10^{18} \text{ cm}^{-3}$	14.7	1.7	2
Pump region width $W_0/\mu\text{m}$	8.0	6.0	6.0
Amplifier length L/cm	0.07	0.07	0.14
Effective beam size in the heterostructure layer plane $w/\mu\text{m}$	10	6.0	6.0
Saturation intensity $I_s/10^5 \text{ W cm}^{-2}$	5.84	2.34	2.34
Transparency current J_{tr}/mA	106	9	22
Mode phase–amplitude coupling coefficient R_1	12	3	5
Active-region thickness d_a/nm	8	8	8
Master oscillator wavelength λ_0/nm	850	850	850
Carrier spontaneous recombination time τ/ns	1.0	1.0	1.0
Optical confinement factor Γ_x	0.02	0.02	0.02
Effective beam size in the direction perpendicular to the heterostructure layers $d \approx d_a/\Gamma_x/\mu\text{m}$	0.4	0.4	0.4

problem in the (yz) plane, in which optical beams are added. This approach is justified by the fact that the transverse spatial distribution of wave amplitude for diode lasers is factorised relative to the transverse axes x and y in the overwhelming majority of cases. Since the transverse field amplitude distribution along the x axis from the sum of beams coincides with the amplitude distribution from one beam, the field amplitude distribution along the x axis will not be considered. We proceed from the fact that the output radiation power for each zigzag is P_0 , with a Gaussian intensity distribution (along the y axis) outside (near the bar output face). In this situation, the amplitude of output electromagnetic wave in the scalar approximation will be approximated by a component of magnetic field strength H_j^x along the x axis for the j th zigzag:

$$H_j^x(y, z) \approx A \exp\{i[\beta z \cos \varphi_0 + \beta(y \sin \varphi_0 - D(j-1)) + \xi_j] - [(y - D(j-1)) \cos \varphi_0 / w]^2 / 2\}, \quad (4)$$

where

$$A = \left(\frac{8\sqrt{\pi} P_0 \cos \varphi_0}{c w d_{\text{eff}} \cos \varphi_m} \right)^{1/2}; \quad \varphi_m = \arcsin(\beta \sin \varphi_0 / k_0)$$

is the tilt angle of the beam axis in free space (Fig. 2), $\beta = k_0 n_{\text{eff}}$ is the propagation constant for the waveguide mode in the diode bar, n_{eff} is the effective refractive index, ξ_j is the constant component of beam phase for the j th zigzag, $P_0 = (1 - r) u I_s d_{\text{eff}} w$, $d_{\text{eff}} = d_a / \Gamma_x$ is the effective transverse size of optical beam along the x axis, Γ_x is the optical confinement factor along the x axis, and k_0 is the wave vector modulus in vac-

uum. Distribution (4) is the most typical case of approximation of the fundamental transverse mode with TE polarisation.

With allowance for the aforesaid, the total distribution of the output wave amplitude along the entire diode bar for $z = +0$ takes the form

$$H_0(y) \approx A \sum_{j=1}^N \exp\{-[y - D(j-1)]^2 \cos^2 \varphi_0 / 2w^2\} \times \exp\{i[\beta(y - D(j-1)) \sin \varphi_0 + \xi_j]\}. \quad (5)$$

The intensity distribution in the far-field zone can be found using the Stratton–Chu formula [14] for a distant point (x_0, y_0, z_0) . As a result, we arrive at

$$H(y_0) \approx \frac{ik_0 \cos \varphi_m}{2\pi} \int_{-\infty}^{\infty} \frac{\exp(ik_0 \tilde{R})}{\tilde{R}} H_0(y) dx dy, \quad (6)$$

where \tilde{R} is the distance from bar surface points to the distant point. Having introduced a local coordinate \tilde{y} according to the equality $y = D(j-1) + \tilde{y}$ and using the standard approach [15], we transform (6) into the expression

$$H(y_0) \approx \frac{A(i-1) \cos \varphi_m}{2} \sqrt{\frac{k_0}{\pi \tilde{R}_0}} \sum_{j=1}^N \int_{-\infty}^{\infty} \exp(-\tilde{y}^2 \cos^2 \varphi_0 / 2w^2) \times \exp(ik_0 \tilde{R}) \exp[i(\beta \tilde{y} \sin \varphi_0 + \xi_j)] d\tilde{y}, \quad (7)$$

where \tilde{R}_0 is the distance from the origin of coordinates to the distant point. Thus, we obtain the expression for the output-power angular distribution $I(\varphi)$:

$$I(\varphi) \approx \frac{P_0 k_0 w \cos \varphi_m}{\cos \varphi_0 \sqrt{\pi}} f(\varphi_0, \varphi) \times \left| \sum_{j=1}^N \exp[ik_0 D(j-1) \sin \varphi + i\xi_j] \right|^2. \quad (8)$$

Here $f(\varphi_0, \varphi) = \exp[-(\beta \sin \varphi_0 - k_0 \sin \varphi)^2 w^2 / (\cos^2 \varphi_0)]$ is the envelope of the general directional pattern. The maximum $f(\varphi_0, \varphi)$ value is obtained for the angle $\varphi = \varphi_m$, satisfying the refraction law on the diode bar output face.

When analysing (8), we should note the following. To implement coherent combining of all beams for any chosen angle $\varphi = \tilde{\varphi}$, one must choose an appropriate ξ_j^0 value (the output-wave phase difference) by varying the currents in the first two sections in each zigzag so as to make valid the equality

$$k_0 D j \sin \tilde{\varphi} + \xi_j^0 = 2\pi m_j, \quad (9)$$

where m_j is an integer. Based on Eqn (8), one can easily find analytically $I(\varphi)$ for

$$\varphi = \tilde{\varphi} + \Delta\varphi, \quad (10)$$

where the angle $\tilde{\varphi}$ satisfies Eqn (9). For example, a possible value is $\tilde{\varphi} = \varphi_m$. In this case, we obtain the following expression for $I(\varphi)$:

$$I(\Delta\varphi) \approx \frac{P_0 k_0 w \cos \varphi_m}{\cos \varphi_0 \sqrt{\pi}} F(\Delta\tilde{\varphi}) \times \frac{\sin^2[(N\Delta\tilde{\varphi}k_0 D \cos \varphi_m)/2]}{\sin^2[(\Delta\tilde{\varphi}k_0 D \cos \varphi_m)/2]}, \quad (11)$$

where

$$F(\Delta\tilde{\varphi}) = \exp\left[-\left(\frac{k_0 w \Delta\tilde{\varphi} \cos \varphi_m}{\cos \varphi_0}\right)^2\right];$$

$$\Delta\tilde{\varphi} = [\sin(\Delta\varphi) - 2\sin^2(\Delta\varphi/2)\tan \varphi_m] \approx \Delta\varphi.$$

Expression (11) yields an angular distribution $I(\Delta\varphi)$ in the form of a set of lobes with an angular width $\delta\varphi \approx \lambda/(ND \cos \varphi_m)$ and an angular distance $\Phi \approx \lambda/(D \cos \varphi_m)$ between them. The number of these lobes is determined by the envelope of function $F(\Delta\tilde{\varphi})$. It can be seen that the intensity in each lobe increased by a factor of N^2 in comparison with the case of a single amplifier. However, with allowance for the fact that the total power also increased N times, the brightness of the total beam (obtained by coherent combining), increased, as was suggested initially, by a factor of N . Obviously, an additional introduction of a regular phase shift of the output wave for the j th zigzag by $\Delta\xi_j = \pm j\pi s k_0 D \cos \varphi_m / N$, where s lies in the range $-N < s < N$, should lead to a shift of all directional pattern lobes by an angle $\Delta\varphi$ in the range $-\Phi/2 < \Delta\varphi < \Phi/2$.

The above analytical result refers to the ideal case of exact adjustment of output-wave phases by varying ξ_j up to the values ξ_j^0 satisfying (9). In reality, there always may be (and are) random deviations $\delta\xi_j$ from exact adjustment. A numerical simulation of directional pattern makes it possible to determine quantitatively the degree of influence of these random

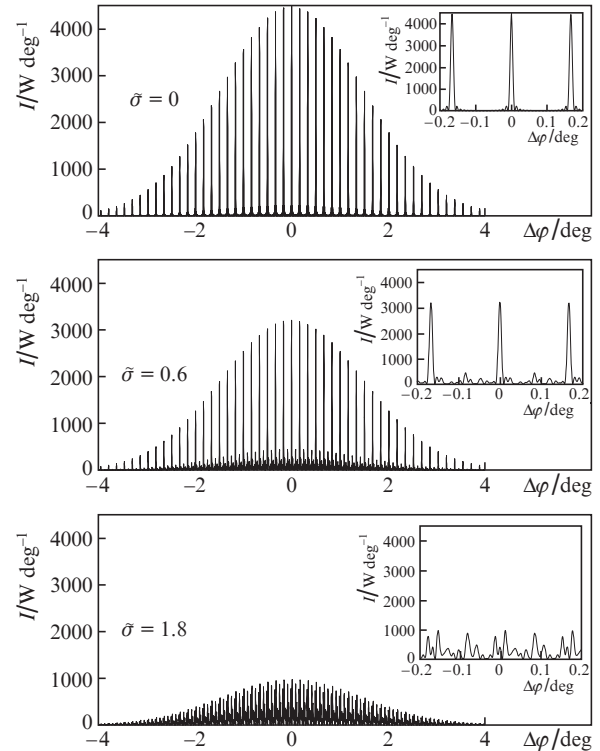


Figure 4. Influence of phase fluctuations in the output radiation from segments of a zigzag amplifier on its directional pattern at coherent combining of output beams. The parameter σ is the mean-square phase deviation for segment output radiation from the target phase value. The section tilt angle is 6° , the amplifier width is 1.5 mm, the output power of each segment is 1 W, and the number of segments is 16. The other parameters are listed in Table 1. The insets show fragments of the corresponding directional patterns with enlarged angular resolution.

deviations. Figure 4 shows the results of calculating the directional pattern using formula (8). The role of parameter $\tilde{\sigma}$ for the curves was played by the random phase deviation $\delta\xi_j$ from exact adjustment in the form

$$\xi_j = \xi_j^0 + \delta\xi_j, \quad \tilde{\sigma} = \sqrt{\delta\xi_j^2}. \quad (12)$$

Figure 4 demonstrates that, at $\tilde{\sigma} < 0.6$, the intensity in the maximum decreases by no more than 30% in comparison with the case of exact adjustment. The condition $\tilde{\sigma} < 0.6$ can be considered as a requirement and some criterion for the accuracy of phase adjustment in output beams.

The modern level of technology makes it possible to integrate more than 20 diode amplifiers in one diode bar. Currently, the attainable brightness level for one amplifier [10, 16] is $\sim 10^9$ W cm⁻² sr⁻¹ at a power of ~ 1 W. Thus, one would expect coherent combining to yield a brightness level of $\sim 10^{10}$ W cm⁻² sr⁻¹ and, correspondingly, output power of ~ 20 W in our case.

Obviously, this is valid for only the case where the uncontrolled phase shift is $\delta\xi_j \equiv 0$, i.e., when exact beam phasing occurs. If the mean-square phase deviation in the beams has a finite value $\xi_j^2 = \tilde{\sigma}^2$, the additive to the total-beam brightness as a result of coherent combining decreases by a factor of $\exp(-\tilde{\sigma}^2)$ in comparison with the case of exact phasing.

3. Conclusions

It was shown that coherent combining of optical beams in a diode amplifier with a zigzag optical axis can be used to increase multiply the total beam brightness with a simultaneous increase in the total radiation power. An essential condition for this procedure is a stable and identical field amplitude distribution, corresponding to one transverse mode, in each output beam. In this context the potential of coherent combining of wide (more than 6 μ m) output beams appears to be limited. For example, when using an output amplifier with an expanding active region [shaped as a horn in the plane of structure layers (y z)] along the optical axis, beam filamentation leads inevitably to uncontrolled transverse (along the y axis) phase deviation, which is equivalent to the occurrence of a random variable $\delta\xi_j$. As a consequence, the total beam brightness may be significantly reduced.

The presence of M lobes instead of one in the directional pattern is related to only the filling factor; i.e., $M = D/w$. This circumstance, which may be inconvenient for practical applications, is not of fundamental importance, because, using passive external optics, one can converge the lobes into one with preservation of total beam brightness.

References

1. Albrodt P., Hanna M., Moron F., Decker J., Winterfeldt M., Blume G., Erbert G., Crump P., Georges P., Lucas-Leclin G. *Proc. SPIE*, **1051**, 105140T (2018).
2. Schimmel G., Janicot S., Hanna M., Decker J., Crump P., Erbert G., Witte U., Traub M., Georges P., Lucas-Leclin G. *Proc. SPIE*, **10086**, 100860O (2017).
3. Zhao Y., Zhu L. *Proc. SPIE*, **8965**, 89650F (2014).
4. Creedon K.J., Redmond S.M., Smith G.M., Missaggia L.J., Connors M.K., Kinsky J.E., Fan T.Y., Turner G.W., Sanchez-Rubio A. *Opt. Lett.*, **37**, 5006 (2012).
5. Redmond S.M., Creedon K.J., Kinsky J.E., Augst S.J., Missaggia L.J., Connors M.K., Huang R.K., Chann B., Fan T.Y., Turner G.W., Sanchez-Rubio A. *Opt. Lett.*, **36**, 999 (2011).
6. Born M., Wolf E. *Principles of Optics: Electromagnetic Theory of Propagation, Interference, and Diffraction of Light* (Oxford: Pergamon, 1964; Moscow: Nauka, 1973).
7. Kawashima T., Kanabe T., Matsui H., Eguchi T., Yamanaka M., Kato Y., Nakatsuka M., Izawa Y., Nakai S., Kanzaki T., Kan H. *Jpn. J. Appl. Phys.*, **40**, 6415 (2001).
8. Prozorov O.N., Rivlin L.A., Yakubovich S.D. *JETP Lett.*, **12**, 190 (1970) [*Pis'ma Zh. Eksp. Teor. Fiz.*, **12**, 282 (1970)].
9. Rivlin L.A. *Sov. J. Quantum Electron.*, **1** (3), 228 (1971) [*Kvantovaya Elektron.*, (3), 34 (1971)].
10. Vysotskii D.V., Elkin N.N., Napartovich A.P., Sukharev A.G., Troshchieva V.N. *Quantum Electron.*, **36** (4), 309 (2006) [*Kvantovaya Elektron.*, **36** (4), 309 (2006)].
11. D'yachkov N.V., Bogatov A.P., Gushchik T.I., Drakin A.E. *Quantum Electron.*, **44**, 1005 (2014) [*Kvantovaya Elektron.*, **44**, 1005 (2014)].
12. Bogatov A.P. *Sov. J. Quantum Electron.*, **17**, 1394 (1987) [*Kvantovaya Elektron.*, **14**, 2190 (1987)].
13. Popovichev V.V., Davydova E.I., Marmalyuk A.A., Simakov A.V., Uspenskii M.B., Chel'nyi A.A., Bogatov A.P., Drakin A.E., Plisyuk S.A., Stratonnikov A.A. *Quantum Electron.*, **32**, 1099 (2002) [*Kvantovaya Elektron.*, **32**, 1099 (2002)].
14. Dmitriev V.I., Zakharov E.V. *Integral'nye uravneniya v kraevykh zadachakh elektrodinamiki* (Integral Equations in Boundary Problems of Electrodynamics) (Moscow: Izd-vo MGU, 1987) p. 93.
15. Landau L.D., Lifshitz E.M. *The Classical Theory of Fields* (Oxford: Pergamon, 1980; Moscow: Nauka, 1988).
16. Sverdlov B., Pfeiffer H.-U., Zibik E., Mohr diek S., Pliska T., Agresti M., Lichtenstein N. *Proc. SPIE*, **8605**, 860508 (2013).